J Nanostruct 11(3): 514-523, Summer 2021

RESEARCH PAPER

SnO_2:Au/Carbon Quantum Dots Nanocomposites: Synthesis, Characterization, and Antibacterial Activity

Ali B. Roomi [1,2], Gunawan Widjaja [3], Dwiana Savitri [4], Abduladheem Turki Jalil [5,6] *, Yasser Fakri Mustafa [7], Lakshmi Thangavelu [8], Galiya Kazhibayeva [9], Wanich Suksatan [10], Supat Chupradit [11], Surendar Aravindhan [12]

[1] *Unviersity of Thi-Qar, Thi-Qar-64001, Iraq*

[2] *Biochemistry and biological engineering research group, Scientific Research Center, Al-Ayen University, Iraq*

[3] *Gunawan Widjaja, Universitas Krisnadwipayana, Jakarta Indonesia*

[4] *Faculty of Medicine, Universitas Lambung Mangkurat, Banjarmasin, Kalimantan Selatan, Indonesia*

[5] *Faculty of Biology and Ecology, Yanka Kupala State University of Grodno, Grodno, Belarus*

[6] *College of Medical Technology, The Islamic University, Najaf, Iraq*

[7] *Department of Pharmaceutical Chemistry, College of Pharmacy, University of Mosul, Mosul-41001, Iraq*

[8] *Department of Pharmacology,saveetha Dental College and Hospital, saveetha institute of medical and Technical Sciences,saveetha university,Chennai,India*

[9] *Toraighyrov University, Pavlodar, Kazakhstan*

[10] *Faculty of Nursing, HRH Princess Chulabhorn College of Medical Science, Chulabhorn Royal Academy, Bangkok, Thailand*

[11] *Department of Occupational Therapy, Faculty of Associated Medical Sciences, Chiang Mai University, Thailand*

[12] *Department of Pharmacology, saveetha dental College and hospital ,saveetha institute of medical and technical sciences,chennai , india*

ARTICLE INFO

Article History:
Received 11 April 2021
Accepted 19 June 2021
Published 01 July 2021

Keywords:
Antibacterial
MBC
MIC
Nanocomposites

ABSTRACT

Carbon quantum dots-based nanostructures have been found more attention in recent years. In this study, Au-doped tin oxide/carbon quantum dots (Au:SnO_2/carbon quantum dots) nanocomposites was prepared via simple and friendly to the environment route. The obtained results from X-ray diffraction (XRD) analysis, Fourier-transform infrared spectroscopy (FT-IR), scanning electron microscopy (SEM), energy dispersive spectroscopy (EDS) analysis, photoluminescence spectroscopy (PL), and Ultra violet-Visible (UV-Vis) spectroscopy showed the formation of the pure and regular shape of Au:SnO_2/ carbon quantum dots. Then, prepared Au:SnO_2/ carbon quantum dots was utilized for the testing of antibacterial activity using Aspergillus niger,, Bacillus subtilis, Candida albicans, Escherichia coli, Klebsiella pneumonia, pseudomonas aeruginosa, Salmonella paratyphi-A serotype, Shigella dysenteriae, Staphylococcus aureus, Staphylococcus epidermidis, and Streptococcus pyogenes. The modified sample showed significant improvement against tested bacteria. The best antibacterial activity was observed in Au:SnO_2/ carbon quantum dots against pseudomonas aeruginosa with MIC values of 62.5 µg/ml. The obtained results demonstrate Au:SnO_2/ carbon quantum dots nanocomposites are highly suitable as an antibacterial agent against both Gram-negative and Gram-positive bacteria.

How to cite this article
Roomi A. B,Widjaja G, Savitri D et al. SnO2:Au/Carbon Quantum Dots Nanocomposites: Synthesis, Characterization, and Antibacterial Activity. J Nanostruct, 2021; 11(3):514-523. DOI:10.22052/JNS.2021.03.009

* *Corresponding Author Email: dr.ali_bader@alayen.edu.iq*

INTRODUCTION

Bacterial infection is the main cause of chronic infection and death [1-5]. Antibiotics are the preferred treatment for bacterial infections because they are cost-effective and powerful [6-10]. However, some studies have provided direct evidence that the widespread use of antibiotics has led to the emergence of multi-drug resistant strains [11-14]. Most of the current molecular antibiotics have an effect on microorganisms via one among the three microorganism targets: cell wall, change of location machinery, and deoxyribonucleic acid replication [15, 16]. Although nanoparticles (NPs) can react simultaneously through several processes, such as (1) generation of reactive oxygen species (ROS), (2) electrostatic interaction with cell membranes, (3) release of ions e (4) internalization [17-20]. Due to the unique properties of nanoparticles due to their size, nanostructures are widely used in antibacterial applications. It is necessary to acknowledge that whereas some metals, akin to copper, tin, and silver, exhibit antibacterial mechanisms in their bulk type, different materials, such as iron oxide, don't seem to be antibacterial in their bulk form however might exhibit antibacterial properties in nanostructure form [21-26]. Tin compound (SnO_2) is one of the notable metal oxides that possess glorious electrochemical, optical and electronic properties. For their excellent properties, SnO_2-based nanomaterials have found more attention in antibacterial application [27-31].

Eduardo B. Tibayan Jr et al. synthesized silver/tin oxide (Ag/SnO_2) nanocomposites as coating materials with high antibacterial activity. They applied scanning electron microscope (SEM) and density functional theory (DFT) methods to characterize the nanocomposite structures and confirm that Ag (1 1 1) and SnO_2 (1 1 0) form nanorods of Ag/SnO_2. They found that toxicity to E. coli and S. aureus increased with respect to the amount of silver within the composite, with the best antibacterial activity being observed at a 4:1 ratio of $Ag:SnO_2$. Also, the antimicrobial activity of the Ag/SnO_2 were increased when particle sizes were reduced to nanoscale [32].

A. Arfaoui et al. prepared SnO_2, SnO_2/MoO_3, and SnO_2/WO_3 thin films via the thermal evaporation technique. They characterized prepared thin films via XRD, AFM, SEM, and UV-Vis analysis. It is found that SnO_2/MoO_3 and SnO_2/WO_3 nanomaterials showed higher photocatalytic activity than of SnO_2. The antibacterial activity investigation towards Pseudomonas Aeroginosa revealed that only SnO_2/WO_3 thin film has shown antibacterial activity[33].

This study aimed to examine the effect of $Au:SnO_2$/carbon dots nanocomposites in preventing bacterial growth. First, $Au:SnO_2$/carbon dots nanocomposites is synthesized via novel and simple route. The structural properties of prepared samples are characterized via XRD, FTIR, EDS, SEM, TEM, UV-Vis, and PL analysis. The antibacterial activity of $Au:SnO_2$/carbon dots nanocomposites is examined against various Gram-negative and Gram-positive bacteria.

MATERIALS AND METHODS

Synthesis of carbon dots

Pears were used to greenly synthesize carbon quantum dots by the hydrothermal method. First, 10 mL of pear water was added to 10 mL ethanol. Then, the prepared solution was placed on the magnetic stirrer for 30 minutes. The obtained solution was transferred into stainless steel autoclave and heated for 5 hours at 190 °C. Finally, the solution was centrifuged several times and keep in the 4 ˚C for further tests.

Synthesis of SnO_2 nanoparticles

Rosemary plant extract was used for the green synthesis of tin oxide nanoparticles. First, 10 mL of the extract was distilled in 20 ml of deionized water. Then, the $SnCl_2.2H_2O$ was distilled in 30 ml of water, then after 20 minutes the Rosemary plant extract solution was added to the tin-containing solution and brown-colored precipitate was obtained. Using a centrifuge, the solid was separated and washed with water. The obtained solid was dried for 12 hours at 60 ˚C. The prepared solid was calcined for 3 hours at 450 °C to formation pure SnO_2 nanoparticles.

Synthesis of $Au:SnO_2$

$Au:SnO_2$ nanomaterial was synthesized similar to the preparation of SnO_2 nanoparticles, except that before adding Rosemary plant extract, $HAuCl_4.3H_2O$ was added to the solution.

Synthesis of $Au:SnO_2$/carbon dots nanocomposites

0.1 g of as-obtained $Au:SnO_2$ nanoparticle was dissolved in 20 cc of distilled water, then 5 cc of the prepared dot was added to the $Au:SnO_2$ nanoparticle mixture. The obtained mixture was

stirred for 24 h vigorously. Finally, the solid was dried for 12 hours at 60 ˚C.

Antimicrobial activity assay

For the antimicrobial activity test, a concentration of 10 mg/ml Au:SnO_2/carbon dots was prepared, then the bacterial suspensions were diluted to 10^6 CFU / ml and finally exposed to treatment with 300 µl Au:SnO_2/carbon dots for 1, 2, 3 and 4 days at 37 ° C. Aliquots (10 µl) were taken from each sample tube, diluted to 10^3 CFU / ml and seeded on Müller agar Hinton for 24 to 37 ° C. The colonies were then counted and the results were reported as log10 CFU/ml expressed.

RESULTS AND DISCUSSION

Fig. 1 shows XRD pattern of prepared Au:SnO_2/ carbon dots. As can be seen in XRD pattern, the noisy broad weak peak in 2θ=21˚ have corresponded to carbon dots. Other observed peaks confirmed the formation of tetragonal SnO_2 with space group $P_{42/mnm}$ (reference code 01-077-0450). The high intensity of peaks confirms a good crystallinity of the synthesized tin oxide nanoparticles, and large width of the full width at half maximum (FWHM) of the peaks leads to the small grain size of the tin oxide nanoparticles. For the calculation of crystalline size, the Scherer equation can be applied:

$$Dc = K\lambda/\beta Cos\theta \quad (1)$$

that β is defined as the width of the provided diffraction peak at its half maximum intensity (FWHM), K is the shape factor, which takes a value of about 0.9, and λ is the X-ray wavelength (CuKα radiation, equals to 0.154 nm). The average crystallite size was calculated 23.2 nm. It was predictable that the Au-related peak would not be seen in the XRD patern because the amount of doped Au was very low.

The EDS analysis was applied for the chemical characterization of samples. As well as shown in Fig. 2, the EDX profile virtually proves the presence of C, Sn, O, and Au elements, which might be a part of the authentic synthesized Au:SnO_2/carbon dots. Percentage compositions of the elements present in Au:SnO_2/carbon dots are presented in a Table inserted under Fig. 2. It is clear that no other dominated peak was observed in the EDS spectrum that confirmed that the as-prepared Au:SnO_2/carbon dots is formed with any impurity.

FT-IR analysis was used for the investigation surface functional group of the product. Fig. 3 shows FT-IR spectrum of Au:SnO_2/carbon dots. As-showed broad peak in 3412 and sharp peak

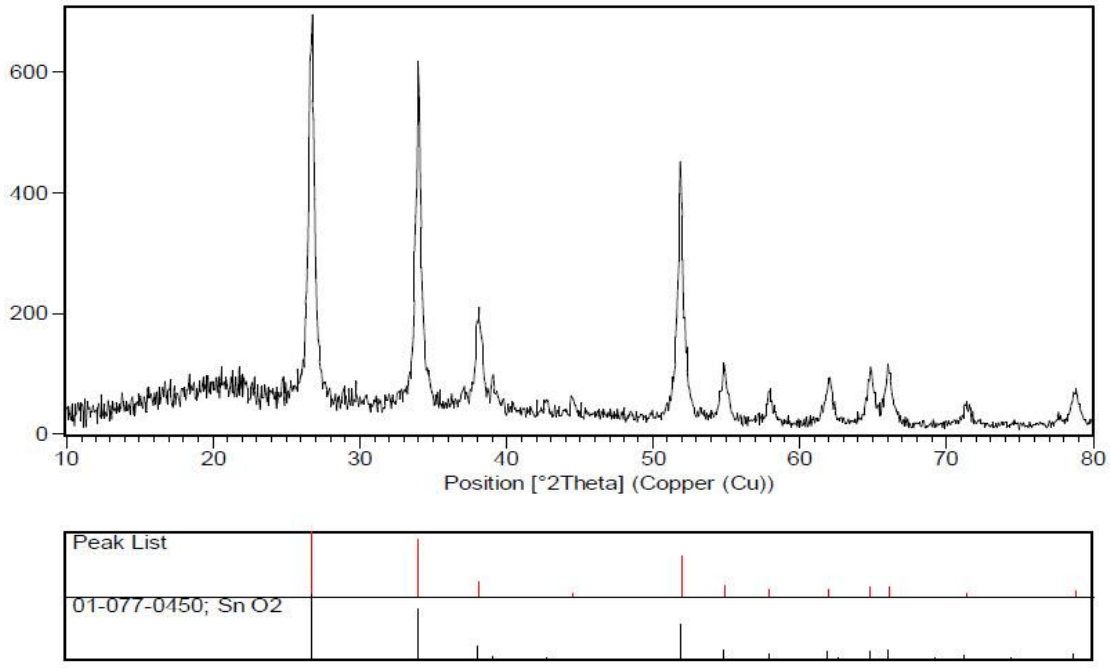

Fig. 1. XRD pattern of synthesized Au:SnO_2/carbon dots nanocomposites.

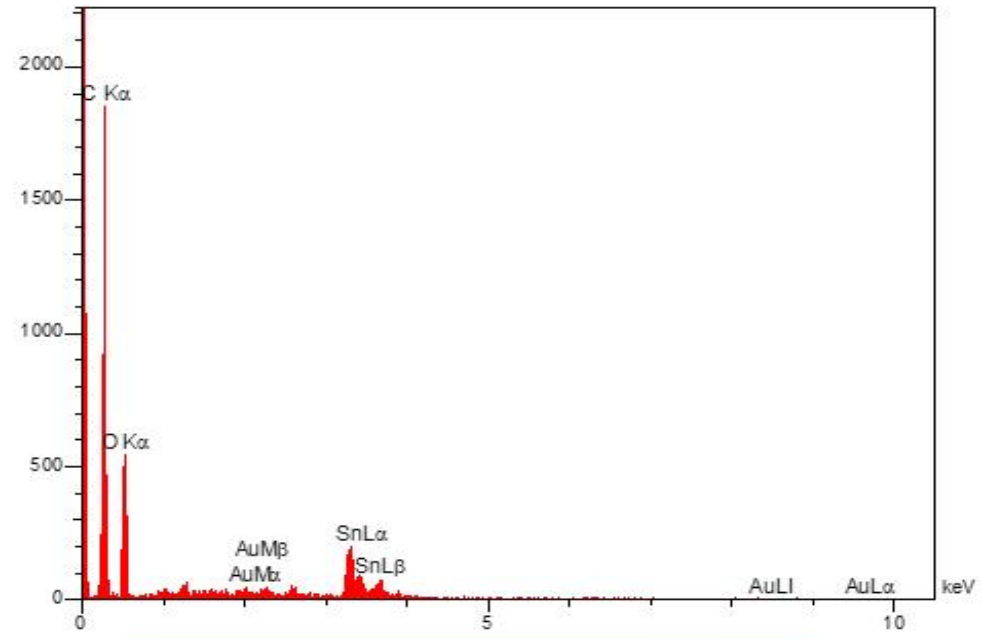

Fig. 2. EDS analysis of as-prepared Au:SnO_2/carbon dots nanocomposites.

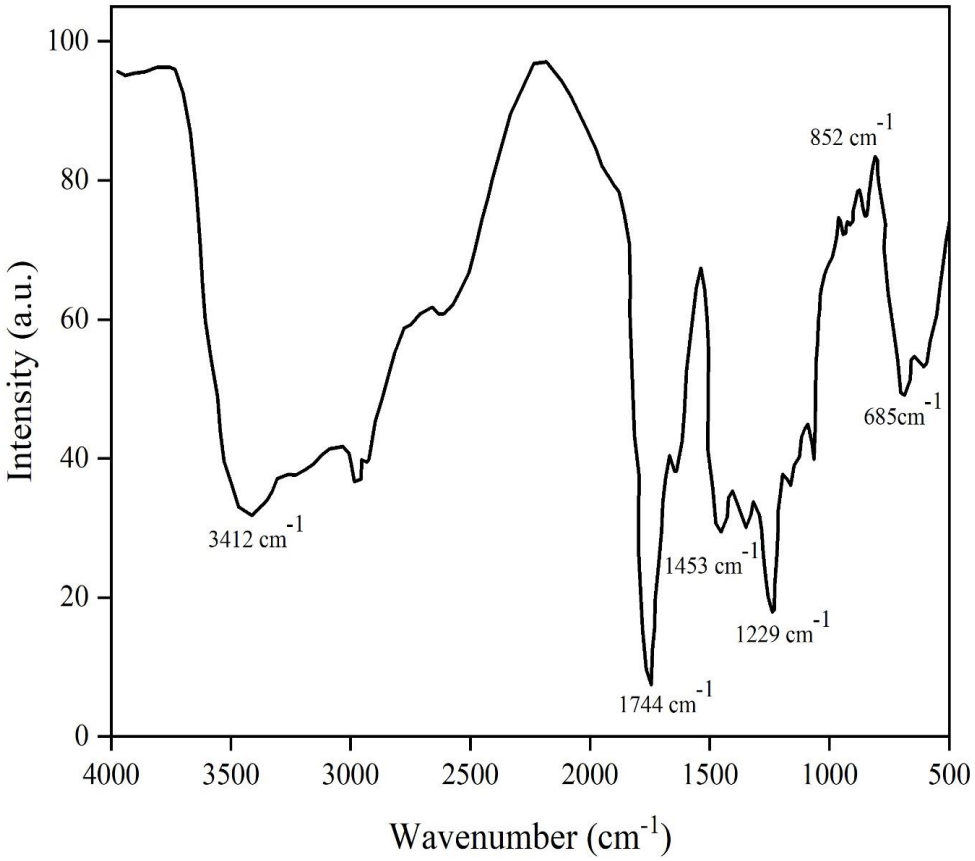

Fig. 3. FTIR spectra of prepared Au:SnO_2/carbon dots nanocomposites.

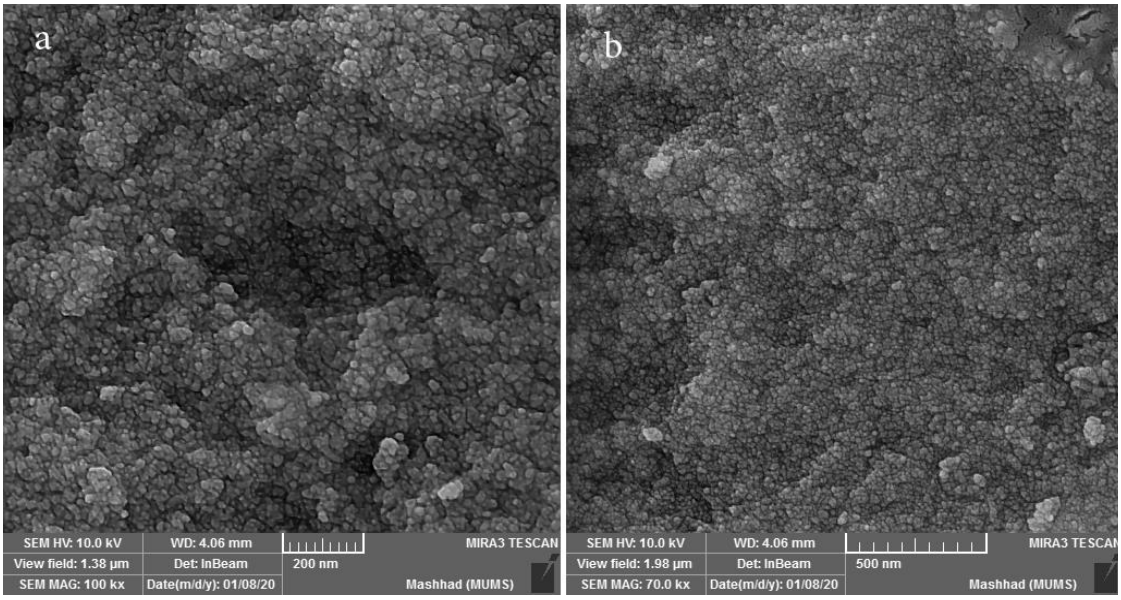

Fig. 4. SEM images of as-prepared Au:SnO_2/carbon dots nanocomposites at two different magnifications.

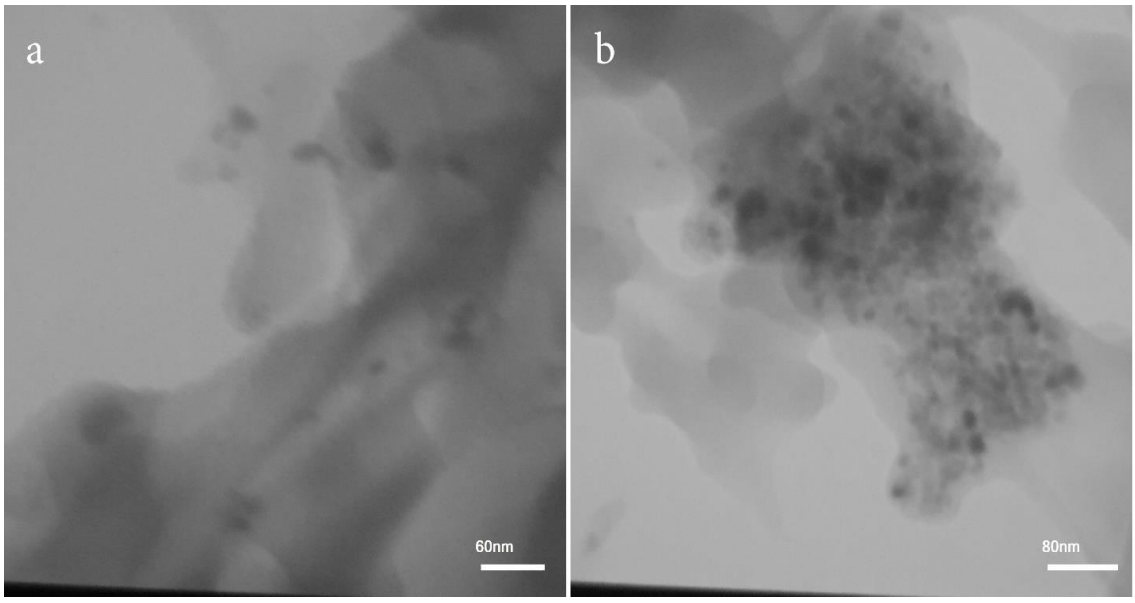

Fig. 5. TEM images of prepared Au:SnO_2/carbon dots nanocomposites at two different magnifications.

at 1744 cm^{-1} in the FT-IR spectrum of products confirm hydroxyl group stretching vibrations and bending mode vibrations associated with the absorption of a few molecules of water. The bonds in the wavenumber range of 1000-1500 cm^{-1} are related to the C-C in carbon dots and Sn-OH stretching vibration. The main characteristic peaks at low wavenumbers, including 685 cm^{-1} and 606 cm^{-1} can be attributed to the antisymmetric and symmetric tin-oxygen-tin vibration, which is derived from the active IR modes E_u (TO) mode and the A_{2u} (TO) mode.

Morphological properties of as-prepared Au:SnO_2/carbon dots nanocomposites were investigated via scanning electron microscope (SEM). SEM images of Au:SnO_2/carbon dots is shown in Fig. 4 at two different magnifications. It can be concluded that the regular morphology of

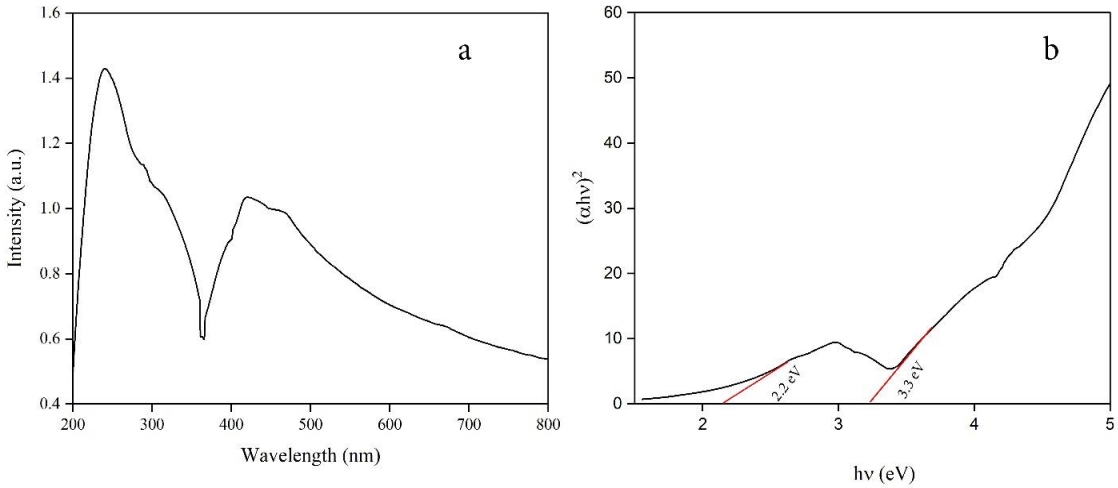

Fig. 6. a) UV-Vis absorption spectra and b) calculated band gap for Au:SnO_2/carbon dots nanocomposites.

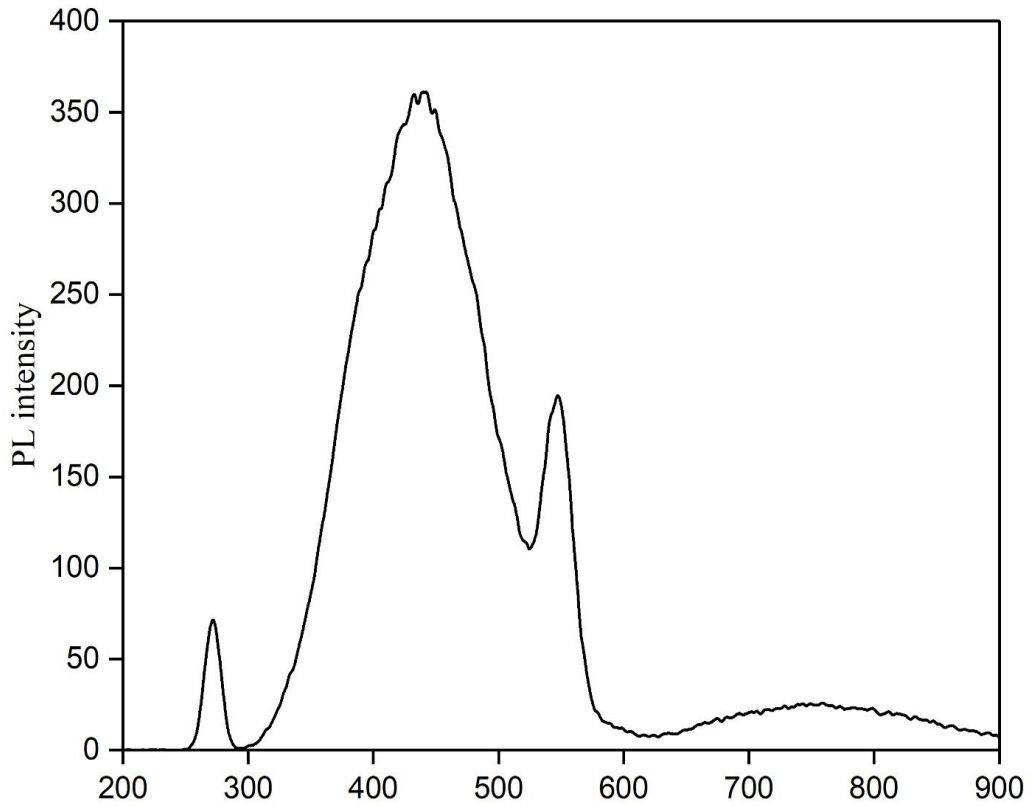

Fig. 7. The photoluminescence spectra of prepared Au:SnO_2/carbon dots nanocomposites.

SnO_2 nanoparticles are formed in 50 nm diameter. It should be noted that SEM images could not distinguish the Au nanoparticles and carbon dots. Carbon dots could not be investigated via the SEM analysis for their very tiny size. For further investigation of prepared Au:SnO_2/carbon dots transmission electron microscopes (TEM) analysis was applied. It is clear in Fig. 5 that very tiny carbon quantum dots are formed with tin oxide nanoparticles. From TEM images, it can be

Table 1. The Minimum Inhibitory Concentration (MIC), Minimum Bactericidal Concentration (MBC), and diameter of inhibition zone of the Au:SnO_2/carbon dots nanocomposites against tested microorganisms.

Test microorganism	SnO_2:Au DD	SnO_2:Au MIC	SnO_2:Au MBC	SnO_2:Au/Cdot DD	SnO_2:Au/Cdot MIC	SnO_2:Au/Cdot MBC
Aspergillus niger (ATCC 9029)		—			—	
Bacillus subtilis (ATCC 6633)		125	>1000	11	62.50	250
Candida albicans (ATCC 10231)		62.50	250		62.50	62.50
Escherichia coli (ATCC 25922)	8	62.50	250	10	125	250
Klebsiella pneumonia (ATCC 10031)		125	1000	11	62.5	250
pseudomonas aeruginosa (ATCC 27853)		62.50	250	10	62.50	125
Salmonella paratyphi-A serotype (ATCC 5702)		62.50	1000	11	62.50	125
Shigella dysenteriae (PTCC 1188)		125	250	11	62.50	62.50
Staphylococcus aureus (ATCC 29737)		250	1000	14	125	250
Staphylococcus epidermidis (CIP 81.55)		250	1000	16	125	250
Streptococcus pyogenes ATCC 19615		62.50	62.50	16	62.50	62.50

revealed that carbon dots have been distributed in Au:SnO_2 homogenously.

The optical properties of prepared Au:SnO_2/carbon dots nanocomposites was investigated via UV-Vis and PL spectroscopy. Fig. 6a shows the UV-Vis absorption spectrum of as-prepared Au:SnO_2/carbon dots in the wavelength range of 200-600 nm. The strong absorption peak is observed at 278 nm. This can be attributed to the direct band gap of SnO_2 nanoparticles that confirms absorption for the electronic transitions from the valence band to the conduction band. The energy band gap (Eg) is calculated from the optical absorption spectra using Tauc relation:

$$(\alpha h\vartheta) = C\,(h\vartheta - Eg)^{1/2}$$

where α is the absorption coefficient, hυ is the photon energy, and Eg is the band gap. As well as illustrated in Fig. 6b, the band gap was determined 2.2 and 3.3 eV for the synthesized Au:SnO_2 and carbon dots respectively. Compared to the previously reported band gaps for SnO_2 and carbon dots, it is found that the calculated band gap is considerable [34, 35]. PL is known as an appropriate technique to investigate optical properties of nanoparticles, the active sites on the surface of metal oxides, the crystalline quality, and also the presence of impurities within the materials further as exciton fine structures. Fig. 7 shows the emission spectrum of prepared Au:SnO_2/carbon dots nanocomposites. The PL spectra of product show the broad luminescence band at 438 and 547 nm. The observed band can be related to the all Sn and oxygen vacancies, Sn interstitials, and defects on the surface of product.

In this study, the antibacterial activity of Au:SnO_2/carbon dots nanocomposites was examined against Gram-positive and Gram-negative bacteria. The broth microdilution procedure were used to determine the MIC and MBC and findings are presented in Table 1. Also, the diameter of the inhibition zone is provided in Table 1. The results demonstrated that Streptococcus pyogenes (ATCC 19615) has the highest sensitivity since the lowest concentration of Au:SnO_2/carbon dots nanocomposites was applied via MIC and MBC value 62.5 and 62.5 µg/ml. The results also revealed the antibacterial effect of Au:SnO_2/carbon dots nanocomposites against other Gram-positive and Gram-negative bacteria. The findings revealed that Au:SnO_2/carbon dots nanocomposites has higher antibacterial activity than Au:SnO_2. No diameter of inhibition zone was observed for Au:SnO_2 nanomaterial against most tested bacteria. Highest antibacterial potency of Au:SnO_2 nanomaterial was observed against Escherichia coli (ATCC 25922) with an inhibition zone of 8 mm. Au:SnO_2/carbon dots showed highest antibacterial activity against Streptococcus

Table 2. The Minimum Inhibitory Concentration (MIC), Minimum Bactericidal Concentration (MBC), and diameter of inhibition zone of some antibiotics against tested microorganisms.

Antibiotics	Rifampin		Gentamicin		Nystatin	
	DD	MIC	DD	MIC	DD	MIC
pseudomonas aeruginosa (ATCC 27853)	—	62.50	22	3.90	NA	NA
Bacillus subtilis (ATCC 6633)	19	31.25	30	3.90	NA	NA
Escherichia coli (ATCC 10536)	10	15.63	23	31.25	NA	NA
Staphylococcus aureus (ATCC 29737)	21	31.25	27	1.95	NA	NA
Klebsiella pneumonia (ATCC 10031)	8	15.63	17	3.90	NA	NA
Staphylococcus epidermidis (ATCC 12228)	44	1.95	39	1.95	NA	NA
Shigelladysenteriae (PTCC 1188)	9	15.36	17	3.90	NA	NA
Proteus vulgaris (PTCC 1182)	8	15.63	24	15.63	NA	NA
Salmonella paratyphi-A serotype (ATCC 5702)	8	15.63	18	3.90	NA	NA
Salmonella enterica subsp. Enterica (ATCC 13076)	17	31.25	—	31.25	NA	NA
Pseudomonas aeruginosa (ATCC 27853)	—	31.25	20	7.81	NA	NA
Enterococcus faecalis (ATCC 19433)	13.5	31.25	125	62.50	NA	NA
Escherichia coli (ATCC 25922)	11	3.90	20	3.90	NA	NA
Staphylococcus aureus (ATCC 25923)	11	1.95	20	1.95	NA	NA
Shigellaflexneri (ATCC 12022)	8	15.63	17	7.81	NA	NA
Proteus mirabilis (ATCC 43071)	9	15.63	20	31.25	NA	NA
Bacillus cereus (ATCC 11778)	17.5	1.95	21	1.95	NA	NA
Staphylococcus epidermidis (CIP 81.55)	27	1.95	45	1.95	NA	NA
Acinetobacterbaumannii (ATCC BAA-747)	8	7.81	17	3.90	NA	NA
Streptococcus pyogenes (ATCC 19615)	21	0.975	32	0.975	NA	NA
Candida albicans (ATCC 10231)	NA	NA	NA	NA	33	125
Aspergillusniger (ATCC 9029)	NA	NA	NA	NA	27	31.2
Aspergillusbrasiliensis (ATCC 16404*)*	NA	NA	NA	NA	30	31.2

pyogenes (ATCC 19615) with an inhibition zone of 16 mm. The improvement of antibacterial activity via introducing carbon dots can be related to the carbon dots-related optical properties. For its semiconductor properties, carbon dots improve optical properties of Au:SnO_2 and this lead to increase the photocatalytic activity of Au:SnO_2/ carbon dots nanocomposites. The presence of carbon dots produced more reactive oxygen species (ROS) and this species lead to increase antibacterial activity. The antibacterial activity of some antibiotics against tested microorganisms is provided in Table 2.

CONCLUSION

In this study Au:SnO_2/carbon dots nanocomposites were synthesized via a simple and novel chemical route. The crystalline structure,

purity, and morphological properties of samples were characterized via XRD, EDS, SEM, and TEM analysis. The results confirmed that Au:SnO_2/carbon dots nanocomposites were formed in pure and regular morphology. The optical properties of products were investigated via UV-Vis and PL analysis. The band gap of as-prepared Au:SnO_2/carbon dots nanocomposites was calculated 2.8 eV. The biological activity of synthesized Au:SnO_2/carbon dots nanocomposites was examined against the Gram-negative and Gram-positive microorganisms. It was found that Au:SnO_2/carbon dots nanocomposites has higher antibacterial activity than Au:SnO_2. . The results revealed that Streptococcus pyogenes (ATCC 19615) has the highest sensitivity since the lowest concentration of Au:SnO_2/carbon dots nanocomposites was applied via MIC and MBC value 62.5 and 62.5 µg/ml.

CONFLICT OF INTEREST

The authors declare that there is no conflict of interests regarding the publication of this manuscript.

REFERENCES

1. Pourhajibagher M, Rahimi-esboei B, Ahmadi H, Bahador A. The anti-biofilm capability of nano-emodin-mediated sonodynamic therapy on multi-species biofilms produced by burn wound bacterial strains. Photodiagnosis and Photodynamic Therapy. 2021;34:102288.
2. Ma Z, Li J, Bai Y, Zhang Y, Sun H, Zhang X. A bacterial infection-microenvironment activated nanoplatform based on spiropyran-conjugated glycoclusters for imaging and eliminating of the biofilm. Chemical Engineering Journal. 2020;399:125787.
3. Simpson ME, Petri WA. TLR2 as a Therapeutic Target in Bacterial Infection. Trends in Molecular Medicine. 2020;26(8):715-717.
4. Yang C, Hu F, Zhang X, Ren C, Huang F, Liu J, et al. Combating bacterial infection by in situ self-assembly of AIEgen-peptide conjugate. Biomaterials. 2020;244:119972.
5. Kamali A, Shokrpour M, Homayuni S, Pazuki S. Comparing the prophylactic effect of ondansetron and dexamethasone in controlling headaches caused by spinal anesthesia among women candidated for caesarean A randomized controlled trial. Electronic Journal of General Medicine. 2018;15(4).
6. Thomsen H, Agnes M, Uwangue O, Persson L, Mattsson M, Graf FE, et al. Increased antibiotic efficacy and noninvasive monitoring of Staphylococcus epidermidis biofilms using per-cysteamine-substituted γ-cyclodextrin – A delivery effect validated by fluorescence microscopy. International Journal of Pharmaceutics. 2020;587:119646.
7. Huijbers PMC, Larsson DGJ, Flach C-F. Surveillance of antibiotic resistant Escherichia coli in human populations through urban wastewater in ten European countries. Environmental Pollution. 2020;261:114200.
8. Ancillotti M, Eriksson S, Andersson DI, Godskesen T, Nihlén Fahlquist J, Veldwijk J. Preferences regarding antibiotic treatment and the role of antibiotic resistance: A discrete choice experiment. International Journal of Antimicrobial Agents. 2020;56(6):106198.
9. Göçmen JS, Ağalar C, Kılıç D, Kaygusuz S, Karabıçak Ç. Antibacterial susceptibility patterns of methicillin resistant staphylococcus spp. from a tertiary reference hospital. Journal of Clinical and Experimental Investigations. 2012;3(1).
10. Nagoba BS, Jahagirdar VL, Davane MS, Aradye SC. Candida species as potential nosocomial pathogens – A review. Electronic Journal of General Medicine. 2018;15(2).
11. Chander AM, Kaur P, Sekhon PK, Kochhar R, Dhawan DK, Bhadada SK, et al. Genome sequence and comparative genomics of multi-drug resistant strain Pseudomonas monteilii CD10_2 isolated from a type 1 diabetic-celiac disease patient. Gene Reports. 2020;20:100734.
12. Lin Y, Li W, Sun L, Lin Z, Jiang Y, Ling Y, et al. Comparative metabolomics shows the metabolic profiles fluctuate in multi-drug resistant Escherichia coli strains. Journal of Proteomics. 2019;207:103468.
13. Gao J, Duan X, Li X, Cao H, Wang Y, Zheng SJ. Emerging of a highly pathogenic and multi-drug resistant strain of Escherichia coli causing an outbreak of colibacillosis in chickens. Infection, Genetics and Evolution. 2018;65:392-398.
14. Khosravanian A, Moslehipour A, Ashrafian H. A review on Bioimaging, Biosensing, and Drug Delivery Systems Based on Graphene Quantum Dots. Progress in Chemical and Biochemical Research. 2021;4(1):44-56.
15. Kapoor G, Saigal S, Elongavan A. Action and resistance mechanisms of antibiotics: A guide for clinicians. J Anaesthesiol Clin Pharmacol. 2017;33(3):300-305.
16. Kohanski MA, Dwyer DJ, Collins JJ. How antibiotics kill bacteria: from targets to networks. Nat Rev Microbiol. 2010;8(6):423-435.
17. Wu H, Yin J-J, Wamer WG, Zeng M, Lo YM. Reactive oxygen species-related activities of nano-iron metal and nano-iron oxides. Journal of Food and Drug Analysis. 2014;22(1):86-94.
18. Yu Z, Li Q, Wang J, Yu Y, Wang Y, Zhou Q, et al. Reactive Oxygen Species-Related Nanoparticle Toxicity in the Biomedical Field. Nanoscale Res Lett. 2020;15(1):115-115.
19. Abdal Dayem A, Hossain MK, Lee SB, Kim K, Saha SK, Yang G-M, et al. The Role of Reactive Oxygen Species (ROS) in the Biological Activities of Metallic Nanoparticles. Int J Mol Sci. 2017;18(1):120.
20. Moslehipour A. Synthesis of a fluorescent mechanochromic polymer based on TGA-capped CdTe Quantum Dots and liquid latex. Advanced Journal of Chemistry-Section B. 2020;2(4):179-186.
21. Wu Z, Xu H, Xie W, Wang M, Wang C, Gao C, et al. Study on a novel antibacterial light-cured resin composite containing nano-MgO. Colloids and Surfaces B: Biointerfaces. 2020;188:110774.
22. Zhang J, Zhu S, Song K, Wang Z, Han Z, Zhao K, et al. 3D reduced graphene oxide hybrid nano-copper scaffolds with a high antibacterial performance. Materials Letters. 2020;267:127527.
23. Ge X, Ren C, Ding Y, Chen G, Lu X, Wang K, et al. Micro/nano-structured TiO2 surface with dual-functional antibacterial effects for biomedical applications. Bioactive Materials. 2019;4:346-357.

24. Wang Z, Liang K, Chan S-W, Tang Y. Fabrication of nano CuAl2O4 spinel for copper stabilization and antibacterial application. Journal of Hazardous Materials. 2019;371:550-557.
25. Marrez DA, Abdelhamid AE, Darwesh OM. Eco-friendly cellulose acetate green synthesized silver nano-composite as antibacterial packaging system for food safety. Food Packaging and Shelf Life. 2019;20:100302.
26. Bakhshkandi R, Ghoranneviss M. Investigating the synthesis and growth of titanium dioxide nanoparticles on a cobalt catalyst. 1393.
27. Pandiyan R, Mahalingam S, Ahn Y-H. Antibacterial and photocatalytic activity of hydrothermally synthesized SnO2 doped GO and CNT under visible light irradiation. Journal of Photochemistry and Photobiology B: Biology. 2019;191:18-25.
28. Faraji M, Mohaghegh N, Abedini A. Ternary composite of TiO2 nanotubes/Ti plates modified by g-C3N4 and SnO2 with enhanced photocatalytic activity for enhancing antibacterial and photocatalytic activity. Journal of Photochemistry and Photobiology B: Biology. 2018;178:124-132.
29. Phukan A, Bhattacharjee RP, Dutta DK. Stabilization of SnO2 nanoparticles into the nanopores of modified Montmorillonite and their antibacterial activity. Advanced Powder Technology. 2017;28(1):139-145.
30. Haskouri S, Cachet H, Duval J-L, Debiemme-Chouvy C. First evidence of the antibacterial property of SnO2 surface electrochemically modified in the presence of bovine serum albumin and chloride ions. Electrochemistry Communications. 2006;8(7):1115-1118.
31. Talebian N, Nilforoushan MR, Zargar EB. Enhanced antibacterial performance of hybrid semiconductor nanomaterials: ZnO/SnO2 nanocomposite thin films. Applied Surface Science. 2011;258(1):547-555.
32. Tibayan EB, Muflikhun MA, Kumar V, Fisher C, Villagracia ARC, Santos GNC. Performance evaluation of Ag/SnO2 nanocomposite materials as coating material with high capability on antibacterial activity. Ain Shams Engineering Journal. 2020;11(3):767-776.
33. Arfaoui A, Mhamdi A, Besrour N, Touihri S, Ouzari HI, Alrowaili ZA, et al. Investigations into the physical properties of SnO2/MoO3 and SnO2/WO3 bi-layered structures along with photocatalytic and antibacterial applications. Thin Solid Films. 2018;648:12-20.
34. Jahnavi VS, Tripathy SK, Ramalingeswara Rao AVN. Structural, optical, magnetic and dielectric studies of SnO2 nano particles in real time applications. Physica B: Condensed Matter. 2019;565:61-72.
35. Salmani E, Rouchdi M, Endichi A, Benchafia E, Ez-Zahraouy H, Hassanain N, et al. The effect of the SnO2 substrate on the band gap and magnetic proprieties of MgH2 ultra-thin films: Ab-initio calculation. Superlattices and Microstructures. 2019;127:27-34.